Online ISSN 1848-3380, Print ISSN 0005-1144
ATKAFF 54(2), 188–198(2013)

Andrzej Sikorski, Marek Korzeniewski

Improved Algorithms of Direct Torque Control Method

DOI 10.7305/automatika.54-2.173
UDK [681.532.5:621.313.333]:519.254
IFAC 2.1.4; 1.1.6

Original scientific paper

In the paper a new way of DTC control method analysis to explain flux and current distortion at a low speed of motor operation is discussed. As a result, a new DTC-δ algorithm is proposed. It is important that the DTC-δ algorithm uses the same switching table as the DTC method. The modified DTC algorithms are free from the disadvantages of the conventional DTC method i.e. hexagonal flux and strongly deformed current at a low speed range. The dynamical properties of the new algorithms are similar to the conventional DTC method. The correctness of the proposed methods has been confirmed by laboratory investigations.

Key words: Direct torque control (DTC), Induction motor drives, Variable-speed drives

Unaprijeđeni algoritmi za izravno upravljanje momentom. Ovaj se rad bavi novim načinom analize izravnog upravljanja momentom (DTC) radi objašnjenja distorzije toka i struje na malim brzinama vrtnje motora. Kao rezultat, predložen je novi DTC-δ algoritam. Pritom je značajno da novi DTC-δ algoritam koristi istu tablicu prekapčanja kao i DTC metoda. Modificirani DTC algoritmi su bez nedostataka karakterističnih za konvencionalne DTC metode, poput heksagonalnog toka i izrazito izobličene struje pri niskim brzinama. Dinamička svojstva novih algoritama su slična konvencionalnoj DTC metodi. Predložene metode su potvrđene laboratorijskim ispitivanjima.

Ključne riječi: izravno upravljanje momentom (DTC), elektromotorni pogoni s kaveznim strojem, pogoni s promjenjivom brzinom vrtnje

1 INTRODUCTION

The method of direct flux and torque control with a switching table (DTC-ST) proposed by Takahashi and Noguchi [1] in 1985 has been used and developed up to now. In the literature on the subject the following problems have been discussed:

- hexagonal flux vector trajectory and distorted stator current at low motor speed,
- motor start-up problems e.g. no possibility of motor "excitation" at the torque set value equal zero,
- variable switching frequency,
- variable torque pulsations.

Modifications of control algorithms are limited because of a limited number of voltage output vectors created by a two level inverter (6 active and 2 zero vectors). Thus, an improvement of one property leads to the deterioration of others. A characteristic feature of the conventional DTC-ST method is that in the steady state three vectors are used (two active and zero vectors) just as in the standard PWM. The only difference lies in the fact that in the standard PWM the switching processes occur in a determined sequence, while in the DTC-ST method, the sequence depends on torque and flux errors. As a result the DTC method should ensure both the minimization of pulsation as well as the switching frequency. These features are needed to improve the drive's technical properties by decreasing speed pulsations and also economical properties by reducing switching frequency which affects power dissipation and inverter efficiency. The main way to improve the DTC method involves the torque pulsation decrease keeping the sampling time t_p and transistors switching frequency unchanged [2, 3]. Constant switching frequency is useful when passive filters are applied on the inverter output. The above is carried out in two ways. One method consists in the use of adequate torque and flux controller structures (using linear controllers) which, in the final stage, take advantage of space voltage modulation. These algorithms are called DTC-SVM [4, 5, 6], due to the fact that the used torque and flux PI controllers, have a longer response time to the torque step changes, although

the complex controller systems [7] bring their properties closer to the DTC method, which applies the nonlinear controllers. The other method involves improving the classical conception of the nonlinear (hysteresis) torque and flux controllers by an introduction of additional modulation algorithms at sampling time t_p [8, 9, 10]. For this purpose additional triangular signals modulating the torque and flux errors are used to decrease pulsations simultaneously increasing the inverter switching frequency. The most advanced algorithms use different level complication predictive controllers [11, 12]. Predictive algorithms require the knowledge of motor parameters that can be best identified on-line. The algorithms are sensitive to parameter changes. Prediction includes accurate calculations of controlled parameters (flux and torque) [13] as well as determination of their values in one or several steps ahead [14, 15, 16].

A better chance of solving DTC-ST problems is offered by multi-level converters, in which a higher number of voltage vectors enable realization of different control algorithms [17].

Frequently, mistakes are made when comparing different algorithms with the DTC-ST standard algorithm analyzing the torque pulsations as the comparisons disregard the average inverter switching frequency. For example, some compare the DTC-SVM method torque pulsation at the same sampling time to the DTC method that uses nonlinear controllers (comparators). It should be kept in mind that during one sampling period t_p the nonlinear controller evokes one voltage vector change, while in DTC-SVM method the PWM modulator evokes six voltage vector changes. Therefore, it is difficult to expect higher torque pulsation in the DTC-SVM method. To be able to compare the pulsations the DTC-ST sampling time t_p should be six times shorter. Obviously, the speed-up requires a faster and more expensive processor [18].

In this paper problems of the hexagonal flux trajectory and current deformations at low motor speed [19, 20] and motor start-up are discussed. Generally, these problems can be solved by predictive algorithms and DTC-SVM (using PWM) algorithms. However, simpler algorithms similar to DTC-ST fail to eliminate these disadvantages. Sometimes mistakes in the creation of algorithms unexpectedly eliminate flux and current distortions in some special conditions. The flux estimation method has a significant effect on the quality of control [6, 21]. It can be shown that a wrong flux estimation resulting in the significant flux phase shift at low speed in some particular cases moves sector border N in such a way that flux and current deformations do not occur at low motor speed. It resembles a part of the algorithm described in section IV. Another mistake is narrowing down of the torque hysteresis at level $dT = 0$. As a result, at low motor speed and large torque error values eT, dT signal take the values of 1 or -1 and a zero vector is not used for $dT = 0$ (Table I).

Table 1: Switching table for the DTC method.

$d\Psi$	dT	N=1	N=2	N=3	N=4	N=5	N=6
1	1	110	010	011	001	101	100
1	0	111	000	111	000	111	000
1	-1	101	100	110	010	011	001
0	1	010	011	001	101	100	110
0	0	000	111	000	111	000	111
0	-1	001	101	100	110	010	011

The analysis of the DTC-ST method has been usually carried out basing on the motor torque equation as a product of stator $\underline{\psi}_s$ and rotor $\underline{\psi}_r$ fluxes and the angle between them as well as the dependence of the stator flux on the inverter output voltage vectors [1, 4]. The analysis is usually carried out in the stationary coordinates $\alpha\beta$. Such an approach, although correct, does not always allow us to notice and to clarify the inconveniences and shortcomings of the DTC method. The author's investigations in the area of analysis and synthesis of the current controlled methods proposed in [22] were used to analyze the DTC method. Although in the DTC method the current components are not controlled directly, interesting conclusions can be drawn concerning the influence of the current components phenomena on the torque and flux values in the DTC method. In the paper analysis of the DTC operation (section III) and also the causes of the current and flux deformation at the low motor speed (section 3.1), are presented.

2 DTC-ST METHOD

The DTC method proposed by Takahashi and Noguchi is based on a direct control of the stator flux and torque. The scheme of the control system is shown in Fig. 1. The stator flux ψ_s and electromagnetic torque T set values (the speed controller output signal) are compared with real values ψ_s and T and passed to the nonlinear controllers (comparators).

The inverter optimal states placed in address memory are selected by a two-level flux comparator and a three-level torque comparator depending on sector N $(\pi/3)$ in which the flux vector is situated. The angle φ_s between the stator flux vector $\underline{\psi}_s$ and α axis in stationary coordinates $\alpha\beta$ is determined by equation: $\varphi_s = \operatorname{arctg}(\psi_{s\beta}/\psi_{s\beta})$. Particular inverter transistor states (converter output voltage vectors) depending on the comparison results of the set and real values of torque and flux and current sector N of flux vector positions are listed in Table I.

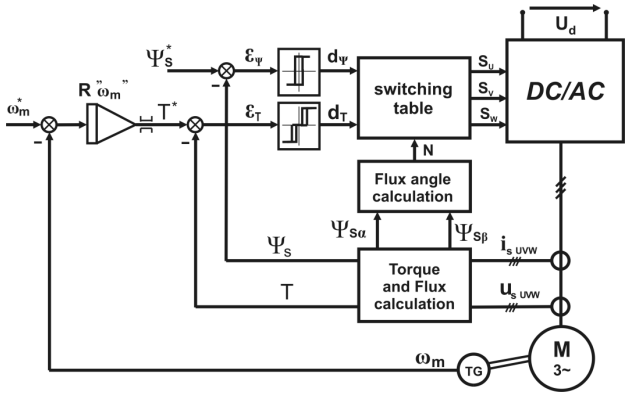

Fig. 1. DTC method control scheme.

3 DTC-ST METHOD ANALYSIS

Although the DTC method is not current controlled, it has some similarities to the field oriented control method (FOC). In both methods flux and torque are controlled, although in the FOC method indirectly by control of current components i_{sd} (proportional to the flux) and i_{sq} (proportional to the torque). The proposed method of analysis views the DTC as the current controlled method [20, 22]. From equations (1) and (2) [20, 22] describing the current derivative ($\underline{K}_{xxx}$ – Fig. 2), which depends on the operation conditions of the drive ($\underline{i}_s$ – motor current, E_s – electromotive force proportional to the motor angular velocity ω_m) and also motor parameters (stator resistance R_s and leakage inductance $L_{\sigma s}$), possible directions of the current vector movement for different inverter voltage vectors are calculated. Both the length and direction of the current derivative corresponding to the voltage vector position in sector $N = 1$ (Fig. 2a) determine the speed and direction of the current vector changes (Fig. 2c).

$$\begin{aligned} L_{\sigma s}\frac{d}{dt}\underline{i}_s &= -(\underline{E}_s + R_s\underline{i}_s^* + j\omega_o L_{\sigma s}\underline{i}_s^*) + \\ &\quad + \begin{cases} \frac{2}{3}U_d e^{j(k_s\frac{2}{3}-\omega_o t)} \\ \text{"0"} \end{cases} \\ &= -\underline{U}_s^* + \underline{U}_d \end{aligned} \tag{1}$$

where:

$$\underline{U}_s^* = U_{sd}^* + jU_{sq}^* = \underline{E}_s + R_s\underline{i}_s^* + j\omega_o L_{\sigma s}\underline{i}_s^* \tag{2}$$

Figure 2b shows the determining of the set value of voltage vector $\underline{U}_s^*$ to achieve desirable current components i_{sd}, i_{sq} for the required angular motor speed proportional to electromotive force.

The directions of the current vector ($\underline{K}_{xxx}$) movement at given voltage $\underline{U}_s^*$ corresponding to the voltage vectors in sector $N = 1$ (110, 010, 101, 001, 111) are shown

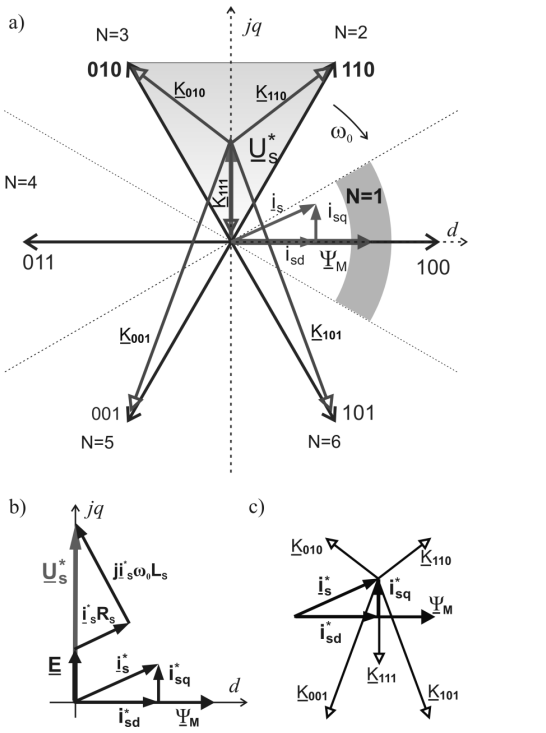

Fig. 2. Graphic illustration of the current vector direction changes $\underline{K}_{xxx}$.

in Fig. 2a. It means that a given inverter voltage vector causes the current vector components to change as shown in Fig. 2c. For example, voltage vector 010 ($\underline{K}_{010}$) causes an increase of current component i_{sq} (torque) and a decrease of current component i_{sd} (flux). The influence of the other vectors on torque and flux changes is presented in Fig. 2c. Since the analysis is performed in rotating coordinates dq then, in accordance with equations (1), (2), the flux, voltage and current vectors are immobile, and the star of the inverter output voltage vectors is rotating. Therefore, only $\underline{K}_{111}$ derivative resulting from the voltage vector (111 or 000) remains unchanged, while the other voltage vectors are variable so their influences are also variable. In the steady state at the "positive" direction speed in sector $N = 1$ only three vectors are used: 111 – when torque is too large, 110 - when torque and flux are too small or 010 – when flux is too large and torque is too small. This can by seen in Fig. 3. All tests were implemented in a laboratory setup in the conditions described in the appendix. The control system was implemented on digital signal processor as DDTC (Discrete Direct Torque Control) structure with zero width of hysteresis and sampling time t_p equal to 67 μs. The flux changes are slow in comparison to the torque changes. During time $t_1 - t_2$ when the flux is too small ($d\psi = 1$) the torque is controlled by the voltage vector 110 – when the torque is too small ($dT = 1$) and by the

voltage vector 111 – when the torque is too large ($dT = 0$).

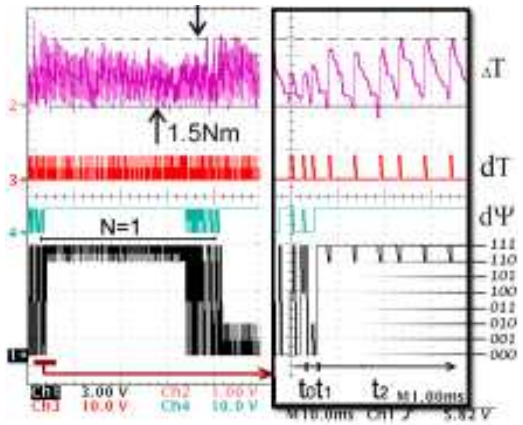

Fig. 3. Torque waveform during the steady state – DTC-ST method.

During time ($t_0 - t_1$), when the flux is too large ($d\psi = 0$), the torque is controlled by the voltage vector 010 – when torque is too small ($dT = 1$) and by the voltage vector 0 (000) – when the torque is too large ($dT = 0$). Vectors 101 and 001 called "dynamic vectors" (in sector $N = 1$) are used during brake and reverse motor states, when the torque set value is significantly less than the torque real value ($dT = -1$).

3.1 Analysis of the DTC method at low speed

At low angular velocity ω_o the electromotive force E and the voltage drop leakage inductance $L_{\sigma S}$ are close to zero. According to equation (2) and Fig. 4a the set voltage vector $\underline{U}_S^*$ overlaps voltage drop of resistance R_S. Figure 4b shows the movement directions of current vector ($\underline{K}_{xxx}$) corresponding to the voltage vectors used in this sector, at the initial moment, when the flux vector goes into sector $N = 1$. At this time (Fig. 4b) three derivatives $\underline{K}_{010}$, $\underline{K}_{110}$, $\underline{K}_{111}$, corresponding to the voltage vectors 010, 110, 111 cause a decrease of the current component i_{sd}, so the flux decreases as well. In the next stage, until the final moment of the flux vector movement in sector $N = 1$ (Fig 4c), the voltage vector 110 ($\underline{K}_{110}$) causes the flux to increase. Meanwhile zero vector 111 ($\underline{K}_{111}$) causes a non - stop decrease of the current component i_{sd} and flux ψ_M. Laboratory test results confirm correctness of the analysis of the causes of the flux decrease during the initial stage of the flux vector movement in sector $N = 1$ as shown in Fig. 5a. To conclude, we can state that the cause of the flux decrease lies in another type of influence of the zero voltage vector and the active vector 110 on the flux changes different from the one assumed in Table I. In accordance with the assumption the zero voltage vector should be neutral to the flux change whereas in reality it causes decrease of the flux. Similarly, under the influence of 110 vector the flux should increase whereas, to a certain extent, the flux actually decreases. It results from the dependence of the current vector direction $\underline{K}_{111}$ on the position of the voltage vector U_s^* that is near the resistant R_s voltage drop. Due to current component i_{sd} causing flux distortion (changeable flux amplitude), the current vector trajectory is not circular in shape during the steady state operation while electromagnetic torque remains constant (Fig. 5a).

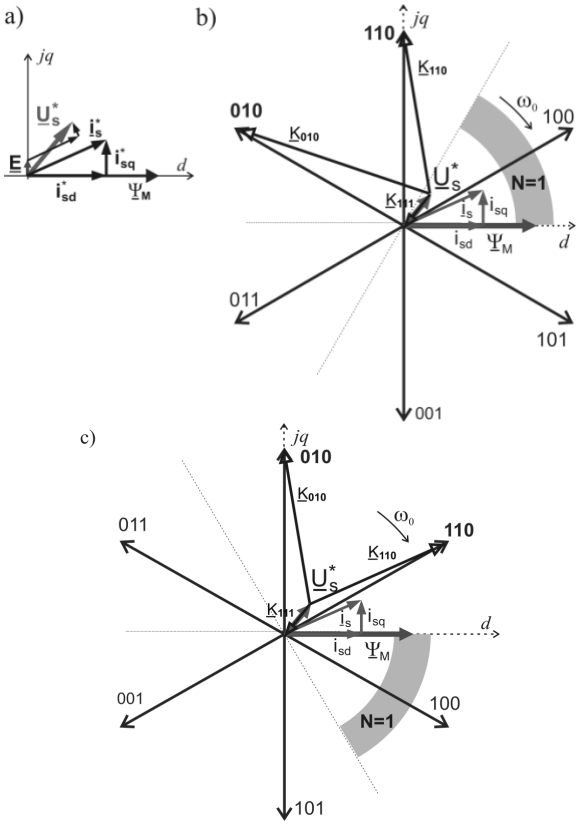

Fig. 4. Graphic illustration of current vector direction changes $\underline{K}_{xxx}$ at low speed range (a) and determination of the current vector movement during initial (b) and final (c) stages of the flux vector movement in sector $N = 1$.

3.2 Motor start-up process controlled by the DTC method

In order to obtain an "excited" motor state ($\psi_M^* = \psi_N$) the nominal flux value ψ_N is set at speed $\omega_m = 0$. In accordance with Fig. 1 $d\psi = 1$ (flux too small) and $dT = 0$, torque is equal to its set value that is equal to zero. In accordance with Table I the zero voltage vector will be chosen (independently of sector N number). As can be seen in Fig. 4 the zero voltage vector does not cause the flux increase i.e. the increase of component i_{sd}, but on the contrary, it causes the decrease of the flux, making it rise to

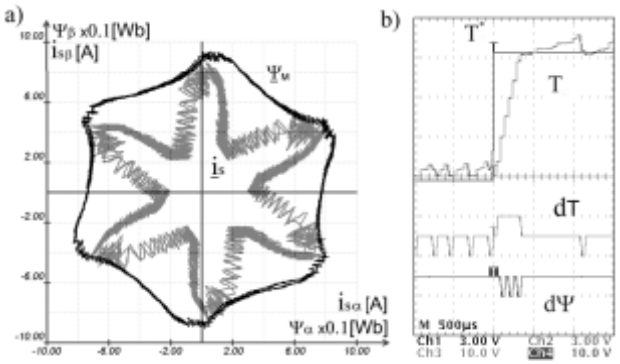

Fig. 5. Results of the laboratory test of the inverter controlled by the conventional DDTC method at low motor speed: flux ψ_M and stator current $\underline{i}s$ trajectories (a) in ab coordinates and the torque waveform during the transient state (b).

the nominal value impossible. Hence it is impossible to "excite" the motor. This situation will not change until the torque set signal becomes different from the zero value, then the active voltage vector will be chosen and in consequence the flux will increase to the set value with the simultaneous increase of the torque (Fig. 6). This process is activated by rapid and simultaneous changes of the flux and torque set values. The following disadvantages of the process can be observed in Fig. 6:

- very long time of the flux increase (longer than the sum of t_1 and t_2),
- slow torque rise to the set value (time t_1),
- no possibility of motor "excitation".

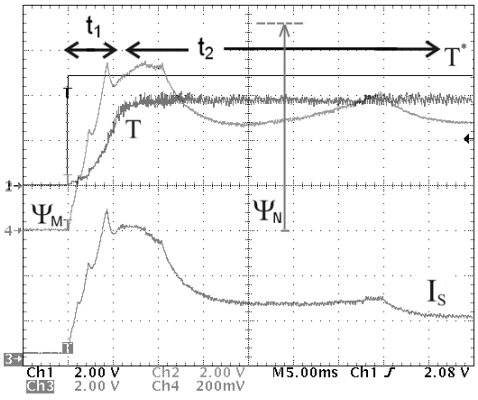

Fig. 6. Current I_s, flux ψ_M and torque T waveforms during motor start-up controlled by conventional the DTC method – results of the laboratory test.

The processes mentioned above have unfavorable influence on the drive system dynamics because the electromagnetic torque fails to increase to the nominal value in a short time. When the electromagnetic torque is equal to its set value ($T = T^*$) and the flux is smaller than its nominal value ($\psi_M < \psi_N$) the motor is overloaded ($I_s > I_N$ – in the time t_2) because of a too slow flux increase. As a result a full control of the torque is not possible during time t_1, when the motor is not sufficiently excited (the flux is too small).

4 DTC-δ ALGORITHM

The disadvantages of the DTC method discussed in the previous sections have led the authors to look for such a solution that would make it possible to use the standard switching table and consequently eliminate the disadvantages of the standard DTC method. In sector $N = 1$ during the steady state the three voltage vectors (010, 110, 000 or 111) are used to control the torque and flux depending on the error values of both control paths. In the steady state the torque control error (in *q*-axis) and the flux control error (in δ-axis) create an error vector moving in the rectangular error area determined by the widths of torque H_T and flux H_ψ hysteresis (Fig. 11).

$$\varepsilon_{\psi T} = \varepsilon_\psi + j\varepsilon_T \tag{3}$$

The necessary operation of turning the error area, described further on in this section, requires rescaling of errors $\varepsilon_T$and ε_ψ to the same scale.

The change of the component lengths related to error vector turning requires keeping their appropriate proportions, which are only possible in the same scale. After the transformation of the errors and an appropriate choice of the widths for H_T and H_ψ, the error area may become square in shape. The rescaling involves determination of proportionality coefficients between torque and current c_T as well as flux and current c_ψ in nominal conditions. Next, using the equations describing the induction motor in rotating coordinates *dq*, it is possible to determine approximate coefficients of proportionality from the equations that take into account motor nominal parameters. If the stator currents are measurable, the easiest way to determine rated current components i_{sqN} i_{sdN} is in nominal conditions, e.g. for rated sinusoidal voltage supply (providing rated flux) and motor loaded by nominal torque T_N. Subsequently, coefficients of proportionality can be determined from the equations taking into account motor rated param-

eters or from approximated equations:

$$c_\psi = \frac{i_{sdN}}{\psi_{mN}} \cong \frac{i_{sdN}}{L_m i_{sdN}} = \frac{1}{L_m} \tag{4}$$

$$c_T = \frac{i_{sqN}}{T_N} = \frac{i_{sqN}}{p_b \frac{3}{2} \psi_{sdN} i_{sqN}} = \frac{2}{3 p_b \psi_{sdN}} \cong \frac{2\omega_{oN}}{3 p_b U_N \sqrt{2}} \tag{5}$$

where: i_{sqN}, i_{sdN} – components of the rated stator current vector in the *dq* coordinate, respectively proportional to nominal motor torque T_N and flux ψ_{sdN} at the nominal voltage U_N characterized by angular frequency ω_{oN}. The rescaled torque and flux error vector can be expressed by the following equation:

$$\varepsilon_{\mathrm{i}\psi\mathrm{T}} = \varepsilon_\psi c_\psi + j\varepsilon_T c_T = \varepsilon_{i\psi} + j\varepsilon_{iT} \tag{6}$$

Table I shows which voltage vector should be used to make the error vector return into the square when it crosses the square border at a specific point. In sector $N = 1$ the appropriate voltage vectors are: vectors 010, 110 and the zero vectors (111 or 000). They are assigned to the error square periphery as shown in Fig. 7c.

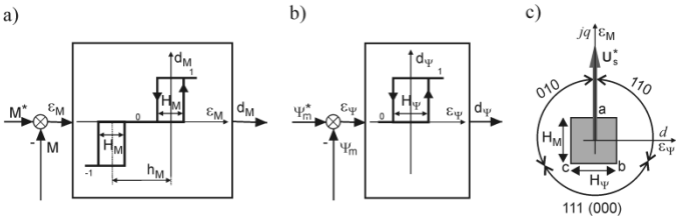

Fig. 7. Error area in conventional DTC method (a) and in DTC-δ method (b)

Looking at the DTC method as voltage and current control we can make following observations. It is assumed in the DTC method that the set value of the motor voltage vector $\underline{U}_s^*$ is perpendicular to the flux vector (Fig. 2ab).

It is true for the operation range at high speed (large $\underline{E}$ value) as shown in Fig. 2b. From the voltage control point of view we can state that voltage vector $\underline{U}_s^*$ (causing the required changes of current components i_{sd}, i_{sq} responsible for torque and flux changes) is formed by 010, 110 and zero vectors. This corresponds to the classical space vector modulation (SVM) of $\underline{U}_s^*$ voltage vector. The problems which occur in the DTC method at low motor speed i.e. hexagonal flux and strongly distorted current (Fig.5a) can be also explained using space vector modulation. Voltage vector $\underline{U}_s^*$ at low motor speed is presented in Fig. 4a. This vector ($\underline{U}_s^*$) deviates from *q*-axis by angle δ. It means that the voltage vector should be formed using vectors 110, 100 and 000 (Fig. 8a). That would involve changes in the switching table (100→ instead 110, 110→ instead 010, etc.) or location changes of sector N in relation to the inverter voltage vectors. The shifting of sector $N = 1$ by angle $-\delta$ (in the opposite direction to the deviation of vector $\underline{U}_s^*$ from *jq* axis) to position $N' = 1$ changes influence of derivatives $\underline{K}_{010}$, $\underline{K}_{110}$, $\underline{K}_{111(000)}$ on current components. While the flux vector moves within the sector $N' = 1$ (Fig. 9), the voltage vector instead 010, etc.) or location changes of sector N in relation to the inverter voltage vectors. The shifting of sector $N = 1$ by angle $-\delta$ (in the opposite direction to the deviation of vector $\underline{U}_s$ remains between voltage vectors 110 and 010 and it can be mapped by them. Analyzing Figs 2 and 9, it can be noted that the directions of current changes $\underline{K}_{010}$, $\underline{K}_{110}$, $\underline{K}_{111(000)}$, vary and, as a result, simultaneously exerting influence on torque and flux changes. For example, vector 110 in Fig. 9c, which should normally increase the value of component i_{sq} (and torque), would, in these conditions, result in its decrease.

Therefore, turning the sectors by angle $-\delta$ will not solve all problems. Figures 8c, 8d show that if the error area is additionally turned by angle δ (i.e. angle deviation of vector $\underline{U}_s^*$ from axis *jq* – Fig. 8c), then relations between the corresponding border sections of the error area and their voltage vectors will remain unchanged. It follows from Figs. 8b and 8d that if the error vector reaches the boundary of the error area between points *b* and *c*, then the derivative $\underline{K}_{111(000)}$, (perpendicular to the side) will direct the error inside error area. The other two derivatives are located as shown in Fig. 2a. This means that vector 110 will move the error vector inside the area from the sector between points *a* and *b*, and vector 010 respectively from the sector between points *b*, *c* (Fig. 8d). It should be noted that the system still works on the same "upper" hysteresis loop (change of the comparator torque d_M between values 1 and 0). By introducing the changes described above, it is possible to shape voltage vector $\underline{U}_s^*$, and consequently the components of currents i_{sd}, i_{sq}, and also the torque and flux, using a standard switching table . These observations made it possible to propose a modification of the scheme for the DTC method (Fig. 10) in accordance with the principles outlined in Fig. 8bd.

As in the standard DTC method, the set values of the main flux ψ_m^* and torque T^* are compared with actual (estimated) values ψ_{md} and T. The errors of both quantities are transformed into the current reference frame (4), (5), (6).

This new method requires identification of angle δ between voltage $\underline{U}_s^*$ and *q*-axis. The calculation of the angle is carried out using (2) and according to Fig. 4a.

$$\delta = arc\ tg \frac{-U_{sd}}{U_{sq}} = \frac{-(R_s i_{sd}^* - \omega_o L_{\sigma s} i_{sq}^*)}{E + R_s i_{sq}^* + \omega_o L_{\sigma s} i_{sd}^*} \tag{7}$$

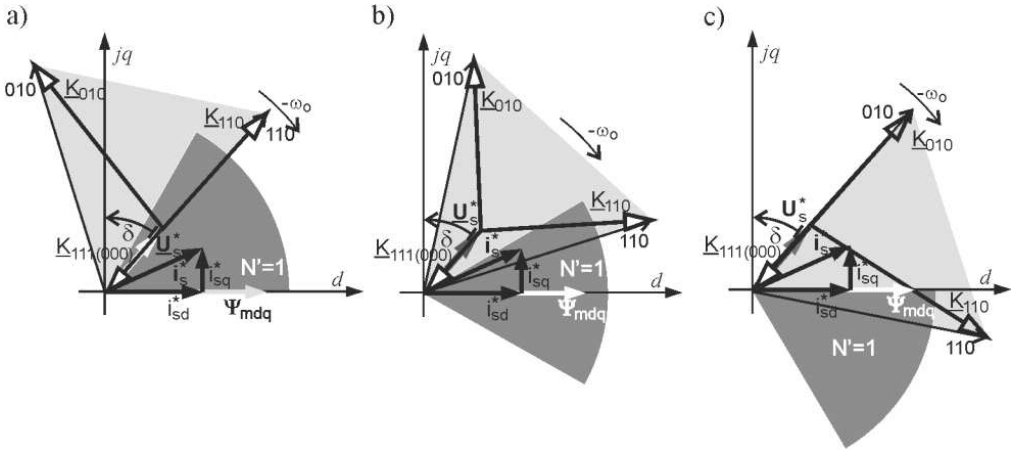

Fig. 9. Creating of $\underline{U}_s^*$ voltage from voltage vectors used in sector $N' = 1$ of the DTC method while flux enters sector $N' = 1$ (a), stays in the center (b) and exits sector $N' = 1$ (c).

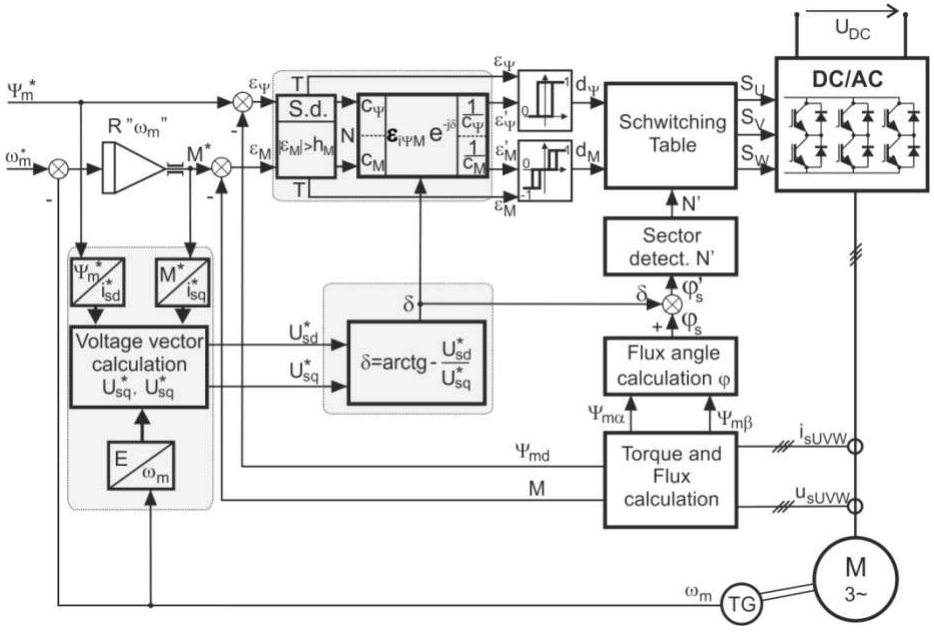

Fig. 10. DTC-δ method control scheme.

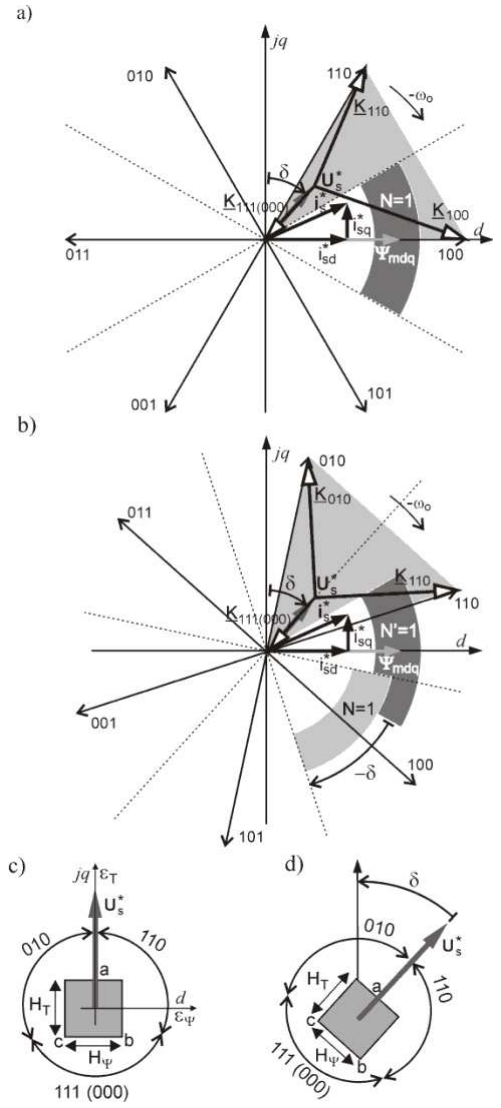

Fig. 8. Illustration of DTC control method modification in rotating reference frame dq at low motor speed – presentation of the current vector direction changes $\underline{K}_{xxx}$ (a) and the current vector direction changes $\underline{K}_{xxx}$ after turning sector $N = 1$ by angle δ (b) Error area in conventional DTC method (c) and in DTC-δ method (d).

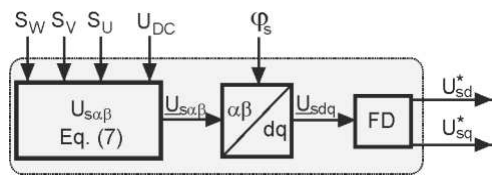

Fig. 11. Calculation model of voltage vector $\underline{U}_s^*$.

The values necessary for the calculation of set current components i_{sd}^*, i_{sq}^* are proportional to the flux ψ_T^* and torque T^* set values (4) (5). The signal proportional to $\underline{E}$ is calculated using the measured mechanical pulsation ω_m. Another way to calculate set voltage $\underline{U}_s^*$ is shown in Fig. 11. It can be determined by filtering the voltages mapped on the basis of switch states and voltage in the DC link circuit.

The output voltage vector in $\alpha\beta$ coordinates is described by the following equation:

$$\mathrm{U}_{s\alpha\beta} = \frac{2}{3} U_{DC} \begin{bmatrix} 1 & \mathrm{a} & \mathrm{a}^2 \end{bmatrix} \begin{bmatrix} S_U \\ S_V \\ S_W \end{bmatrix} \tag{8}$$

After the transformation of equation (8) to the *dq* rotating coordinates and its filtering in the low-pass filter (LF), components U_{sd}, U_{sq} correspond to the components of the vector voltage $\underline{U}_s^*$. The use of both methods of determining $\underline{U}_s^*$ voltage gives almost similar results; however the method presented in Fig. 11 will sometimes give better results in transient states and besides requires no information concerning motor parameters.

Angle δ is used in two transformations. First, it is added to an angle φ_s that determines sectors N borders (Fig. 8b). Secondly, the error area should be turned (Fig. 8d) by angle δ so that it could be possible to keep the relations between adequate sectors of the error area border and the voltage vectors assigned to them. In paper [21] it was demonstrated that the turning of the error area by angle δ is equivalent to the turning of the corresponding error vector $\varepsilon_{i\psi M}$ by angle $-\delta$.

$$\varepsilon'_{i\psi M} = \varepsilon_{i\psi M} \cdot e^{-j\delta} \tag{9}$$

Subsequently, error vector $\varepsilon'_{i\psi M}$ is transferred back to the appropriate scale of flux and torque. This rescaling is necessary when using the width setting of zero level h_T in the torque comparator, the same as in the standard DTC-ST method. Then the errors of both quantities ε'_{ψ} and ε'_{M} are given to comparator controllers. The switching table, in this case, is identical to the DTC-ST method.

Due to the drive quality, transient states such as start-up, braking, reverse, rapid change of torque should be as short as possible. The derivatives of the three voltage vectors used in steady state in the DTC-δ method are the shortest out of 7 possible derivatives. Hence the changes, especially of torque are slow. In transient states (e.g. during braking or reverse at positive speed), when the error fulfils conditions $\varepsilon_M < -h_M$ and $d_M = -1$ (Fig. 7a), we should use the voltage vectors, referred to as "dynamic ones" as their derivatives are the longest and cause the

fastest torque changes. These are either 101 or 001 vectors in sector $N = 1$ depending on the state of comparator d_ψ – Fig. 2a. If angle δ is smaller than $-\pi/3$ (Fig. 12), then the sectors and vectors turned by the angle will make the dynamic vectors work less effectively.

With an increase of angle δ and decreasing speed of the drive, derivatives $\underline{K}_{101}$ and $\underline{K}_{001}$ in particular, will slow down changes of current component i_{sq} responsible for torque changes. A significant impact of dynamic changes in the position of dynamic vectors is observed below speed $0.05\omega_N$. As a result, a mechanisms for identifying the dynamic state (at positive velocity $\varepsilon_M < -h_M$ and $d_M = -1$) where the dynamic vectors are not turned by angle δ (sectors and error vector are not turned). In practice, this means that in the transient state the control process is performed using DTC-ST method. Then the derivatives $\underline{K}_{101}$ and $\underline{K}_{001}$ will be in position as shown in Fig. 2a and will reduce both component i_{sq} and motor torque the fastest. This additional mechanism for determining the dynamic state is essential at low speed. However, its influence will decrease and at $\omega_m > 0.2\omega_N$ the mechanism is practically unnoticeable. Realizing the impact and scope of the extended transient state, it is advisable to consider the need for the identification of the dynamic state and its potential inclusion in the control algorithm.

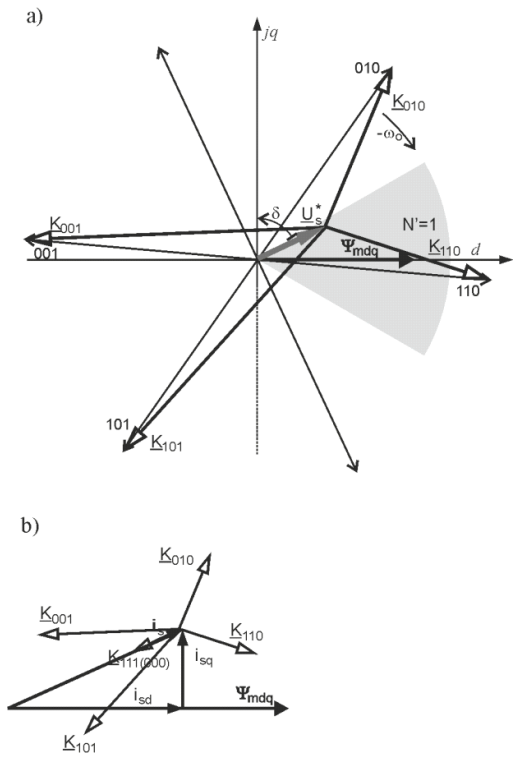

Fig. 12. Location of "dynamic" vectors 001, 101 in sector $N = 1$ at angle $\delta = 65°$ (a) and their effect on the changes of current vector components is (b).

4.1 Laboratory test results of DTC-δ method

The tests were carried out at the frequency of 5 Hz corresponding to 0.1 of the rated value of the motor mechanical pulsation. The flux and current trajectories presented in Fig. 13a are circular in shape, i.e. their waveforms are sinusoidal. The DTC-δ method, independently of the motor speed value, is characterized by full control of flux and torque. It allows us to use this method for motor start-up process eliminating the disadvantages described in section 3.2 connected with the conventional DTC method.

Laboratory tests presented in Fig. 14 confirm the advantages of the method. At time t_1, when the flux rises to its nominal value, the set value of the torque equals zero. The electromagnetic torque at this time oscillates around its set value, and the torque average value is equal to zero. During time t_2 the flux has the nominal value and then the torque set value rises rapidly. During time t_3 the electromagnetic torque is reproduced at the set value level. The stator current achieves the steady-state value very quickly ensuring a very good dynamics of the drive.

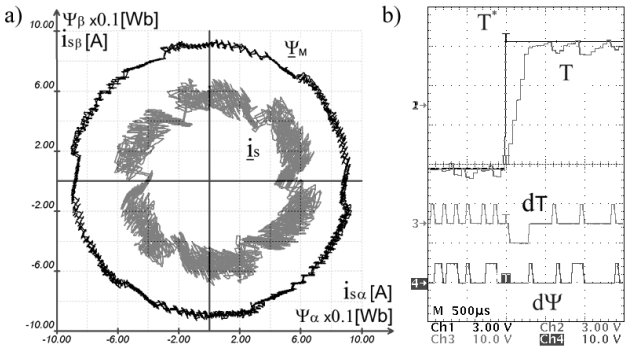

Fig. 13. Flux ψ_M and stator current vectors is trajectories (a) and motor torque waveform during transient states (b) at low speed range - DTC-δ method.

5 CONCLUSION

A new way of DTC method analysis is proposed in the paper. It enables us to effectively identify the problems occurring at low motor speed. The deviation of voltage $\underline{U}_s^*$

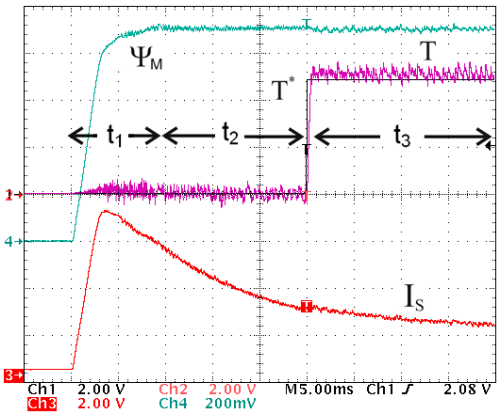

Fig. 14. Current I_s, flux ψ_M and torque T waveforms during motor start-up controlled by the DTC-δ method – results of the laboratory test.

from axis q is a continuous process. Depending on the motor load and speed, angle δ is constantly changing. This means that the correction process should also be continuous and this specific requirement is fulfilled by the DTC method.

A new DTC-δ method eliminating the disadvantages of the conventional DTC method i.e. hexagonal flux vector trajectory and distorted current waveforms, is proposed. The new algorithms keep the dynamic properties of the drive unchanged (Fig. 5b, 13b).

It is particularly important to stress that the proposed DTC-δ method uses the conventional DTC switching table and the correcting mechanisms occur in the whole range of the motor speed changes.

APPENDIX A

The parameters of the IM utilized in this paper are shown in Table II. The DC-voltage of the inverter feeding the IM equals 500V.

Table 2: Induction motor ratings.

P_N [kW]	U_N [V]	I_N [A]	f_N [Hz]	ω_N [rd/s]	Ψ_N [Wb]	R_s [Ω]	R_r [Ω]	$L_{\sigma s}= L_{\sigma r}$ [mH]	L_m [mH]
3.0	400	6.9	50	148	0.9	1.7	1.9	11	162

The control program was implemented in ADSP-21262 with sampling time $t_p = 67\,\mu$s.

The work was supported by The National Centre for Research and Development as a scientific project N R01 002406/2009.

REFERENCES

[1] I. Takahashi and T. Noguchi, "A new quick response and high efficiency control strategy of an induction motor", *IEEE Transactions on Industry Applications*, Vol. IA-22, No. 5, Sep/Oct 1986, pp. 820-827.

[2] J. K. Kang and S. K. Sul, "Analysis and prediction of inverter switching in direct torque control of induction machine based on hysteresis bands and machine parameters", *IEEE Transactions on Industrial Electronics*, Vol. 48, No 3, June 2004, pp. 545-784553.

[3] N. R. N. Idris and A. H. M. Yatim, "Direct torque control of Induction Machines with constant switching frequency and reduced torque ripple", *IEEE Transactions on Industrial Electronics*, Vol. 51, No 4, Aug. 2004, pp.758-767.

[4] G.S. Buja, M.P. Kazmierkowski, "Direct torque control of PWM inverter-fed AC motors-a survey", *IEEE Transactions on Industrial Electronics*, Vol. 51, No 4, Aug. 2004, pp.744-757.

[5] Y. S. Lai and J. H. Chen, "A new approach to direct torque control of induction motor drives for constant inverter switching frequency and torque ripple reduction" , *IEEE Transactions on Energy Conversion*, Vol. 16, No. 3, Sept. 2001, pp. 220-227.

[6] Lascu, I. Boldea and F. Blaabjerg, "Comparative study of adaptive and inherently sensorless observers for variable-speed induction-motor drives", *IEEE Transactions on Industrial Electronics*, Vol. 53, No 1, Feb. 2006, pp.785-792

[7] C. Lascu, I. Boldea and F. Blaabjerg, "Variable-structure direct torque control – a class of fast and robust controllers for induction machine drives", *IEEE Transactions on Industrial Electronics*, Vol. 51, No 4, Aug. 2004, pp.785-792.

[8] Y. S. Lai, W. K. Wang and Y. C. Chen, "A new approach to direct torque control of induction motor drives for constant inverter switching frequency and torque ripple reduction", *IEEE Transactions on Industrial Electronics*, Vol. 51, No 4, Aug. 2004, pp.768-775.

[9] V. Ambrozic, G. S. Buja and R. Menis "Band-constrained technique for direct torque control of induction motor", *IEEE Transactions on Industrial Electronics*, Vol. 51, No 4, Aug. 2004, pp.776-784.

[10] T. Noguchi, M. Yamamoto, S. Kondo and I. Takahashi, "Enlarging switching frequency in direct torque-controlled inverter by means of dithering", *IEEE Transactions on Industry Applications*, Vol. 35, No. 6, Nov/Dec 1999, pp. 1358-1366

[11] T. G. Habetler, F. Profumo, M. Pastorelli, and L. M. Tolbert, "Direct torque control of induction machines using space vector modulation", *IEEE Transactions on Industry Applications*, Vol. 28, No. 5, Sep/Oct 1992, pp. 1045-1053.

[12] M. Bertoluzzo, G. Buja,and R. Menis, "Direct Torque control of an induction motor using a single current sensor", *IEEE Transactions on Industrial Electronics*, Vol. 53, No. 3, June 2006, pp. 778-784.

[13] J. Beerten, J. Verveckken, J. Driesen, "Predictive direct torque control for flux and torque ripple reduction", IEEE Trans. Ind. Electron., vol. 57, no. 1, Jan. 2009,pp. 404-412.

[14] H. Miranda, P. Cortés, J. Yuz, and J. Rodríguez, "Predictive torque control of induction machines based on state space models," IEEE Trans. Ind. Electron., vol. 56, no. 6, pp. 1916–1924, Jun. 2009.

[15] T. Geyer, G. Papafotiou, and M. Morari, "Model predictive direct torque control—Part I: Concept, algorithm and analysis," IEEE Trans. Ind. Electron., vol. 56, no. 6, Jun. 2009 pp., 1894–1905.

[16] G. Papafotiou, J. Kley, K. Papdopoulos, P. Bohren, and M. Morari, "Modelpredictive direct torque control—Part II: Implementation and experimental evaluation," IEEE Trans. Ind. Electron., vol. 56, no. 6, Jun. 2009, pp. 1906–1915.

[17] D. Casadei, G. Serra and A. Tani, "Implementation of a direct torque control algorithm for induction motors based on discrete space vector modulation", *IEEE Transactions on Power Electronics*, Vol. 15, No 4, July 2000, pp. 769-777.

[18] J. N. Nash, "Direct torque control induction motor vector control without an encoder", *IEEE Transactions on Industry Applications*, Vol. 33, Mar/Apr 1997, pp. 333-341.

[19] M. P. Kazmierkowski and A. B. Kasprowicz, "Improved direct torque and flux vector control of PWM inverter-fed induction motor drives", *IEEE Transactions on Industrial Electronics,* Vol. 42, No 4, Aug. 1995, pp.344-350

[20] Sikorski A., Korzeniewski M.: Improved direct torque and flux control of induction motor drive, *COMPEL*, Vol. 26, Nr 4, 2007, s. 1204-1217.

[21] J. Holtz,,"Sensorless control of induction machines – with or without signal injection? *IEEE Transactions on Industrial Electronics*, Vol. 53, No. 1, Feb 2006, pp. 7-30.

[22] A. Sikorski and T. Citko, "Current controller reduced switching frequency for VS-PWM inverter used with AC motor drive application", *IEEE Transactions on Industrial Electronics*, Vol. 45, No. 5, Oct. 1998, pp. 792-801.

Andrzej Sikorski received the M.S. degree in electrical engineering from the Bialystok Technical University, Bialystok, Poland, in 1980 and the Ph.D. degree in electrical engineering from the Warsaw University of Technology, Warsaw, Poland, in 1989. In 1989, he became an Assistant Professor and, in 2000, he became an Associate Professor at the Faculty of Electrical Engineering of the Bialystok Technical University, Bialystok, Poland. His research interests are in the areas of power electronics, particularly AC/DC/AC soft-switching converters and in the control of electrical drives, control of power converters and PWM. He has published more than 80 papers in technical journals and conference proceedings.

Marek Korzeniewski was born in Pisz, Poland In 1975. He received the M.S. degree in electrical engineering, in 2001, and the Ph.D. degree in electrical engineering in 2009 from the Bialystok Technical University, Bialystok, Poland. In 2001 he became an Assistant professor and since 2010 he is Lecturer at the Bialystok University of Technology, Faculty of Electrical Engineering. His research interests are in the areas of power electronics systems, digital control systems run by DSP processors and programmable devices CPLD / FPGA. He has published close to 40 papers in technical journals and conference proceedings.

AUTHORS' ADDRESSES

Prof. Andrzej Sikorski, Ph.D.
Marek Korzeniewski, Ph.D.
Depertment of Power Electronics and Electrical Drivers
Bialystok University of Technology
45D Wiejska St.
15-351 Bialystok, Poland
email: a.sikorski@pb.edu.pl,
m.korzeniewski@pb.edu.pl

Received: 2012-01-19
Accepted: 2012-06-27